International Journal of Nanomedicine

Dovepress
open access to scientific and medical research

Open Access Full Text Article

ORIGINAL RESEARCH

PKH Dyes Should Be Avoided in the EVs Biodistribution Study of the Brain: A Call for Caution

Zheng Wan[1], Tianyi Liu[1], Ning Xu[1], Wenhao Zhu[2], Xiaoyu Zhang[2], Qin Liu[1], Haifeng Wang[2], Honglei Wang[1]

[1]Department of Neurovascular Surgery, The First Hospital of Jilin University, Changchun, Jilin Province, People's Republic of China; [2]Department of Neurotrauma, The First Hospital of Jilin University, Changchun, Jilin Province, People's Republic of China

Correspondence: Haifeng Wang; Honglei Wang, Email hfwang@jlu.edu.cn; wanghongl@jlu.edu.cn

Introduction: Extracellular vesicles (EVs) are nanosized membrane vesicles that are naturally secreted by almost all cells and have gained considerable attention. Many studies have applied EVs to the treatment of brain diseases and validated their effectiveness. Although only a few EVs can penetrate the blood–brain barrier (BBB) into the brain after administration, it has been proven that EVs and their cargos exert their effects by interacting with brain cells. PKH dyes are commonly used to stain EVs for distribution studies. However, systematic investigations of imaging characteristics of the PKH-labeled EVs distributed in the brain are still scarce.

Methods: We stained EVs derived from mesenchymal stem cells with PKH26 or PKH67. PKH26-labeled EVs and PKH67-labeled EVs were administered at the same time into each mouse while PKH26-labeled EVs were given through tail veins and PKH67-labeled EVs were given through intraperitoneal injection. Confocal microscopy was used to explore the distribution difference of two types of EVs given via different routes in the brain.

Results: The fluorescence of PKH26 and PKH67 had nearly identical distributions in brain slices after 1 h, 6 h, 12 h and 1 day of EV administration. Under the same confocal parameters, brain slices without EVs administration demonstrated the same result. However, liver slices from mice administered with labeled EVs showed obviously different distributions of two types PKH fluorescence.

Discussion: These findings raise questions about the ability of PKH dyes as labels for EVs when explore the EV brain distribution observed via confocal microscopy.

Keywords: extracellular vesicles, PKH dyes, brain distribution

Introduction

The interest in the therapeutic function of extracellular vesicles (EVs) for the treatment of human diseases has grown exponentially because of the targeting potential and long-range cell-to-cell communication properties of EVs in the last decade.[1–5] Treatment of neurological disorders is one of the most popular fields of EV studies. Usually, drugs can barely enter the brain, resulting in inferior or no effects on brain diseases because of the blood–brain barrier (BBB), which protects the brain from an unstable external environment and harmful substances. Although only a few EVs can penetrate the blood–brain barrier (BBB) into the brain, it has been proven that EVs and their cargos can interact with multiple brain cells and have therapeutic effects on multiple neurological disorders, such as stroke, brain tumors and Alzheimer's disease.[1,6–8] However, the brain biodistribution of EVs administered by several approaches, such as intravenous, intraperitoneal and intranasal injection, and the major targeting cells in the brain are still unclear. Thus, different methods for labeling EVs have been developed to study the distribution of EVs in the brain. Membrane integration of lipophilic fluorescent dyes is one of the most widely used labeling methods.[9] PKH dyes are highly lipophilic long-chain carbocyanine fluorescent dyes in which the aliphatic tail can rapidly intercalate into the exposed lipid bilayer and form strong noncovalent interactions.[10] PKH dyes are commonly used for the tracking of EVs in different organs because

Received: 23 June 2024
Accepted: 10 September 2024
Published: 26 October 2024

of their simple and convenient characteristics. However, systematic investigations of imaging characteristics of the PKH-labeled EVs distributed in the brain are still scarce. The liver is the most abundantly distributed organ after intravenous or intraperitoneal injection of EVs.[7–9,11] Therefore, to better determine the distribution of PKH-labeled MSC-EVs in the brain, liver samples were also obtained for confocal microscopy. In this article, we found that the fluorescence of PKH-labeled EVs might be confused with spontaneous fluorescence from the brain tissue itself by accidentally observing EVs in the brain through PKH26 and PKH67 fluorescent channels simultaneously. Almost identical distributions of intravenously injected EVs and intraperitoneally injected EVs were shown by confocal microscopy, while the results of PKH fluorescence in the liver after EV administration and in the brain without EV administration further confirmed this phenomenon. Therefore, the use of PKH dyes might not be suitable for the EV tracking in neurological systems.

Material and Methods

Cell Lines and Isolation of EVs

Human amniotic mesenchymal stem cells (MSCs) were obtained from Jilin Zhongke Biological Engineering Cooperation and were authenticated by the China National Institutes for Food and Drug Control (Certification number: SH202100043). Mesenchymal stem cells were maintained in culture media supplemented with 10% heat-inactivated exosome-free fetal bovine serum in a humidified CO2 incubator at 37 °C. MSC culture supernatant was harvested and centrifuged at 1200 rpm for 10 min at 4 °C. A 0.22 μm vacuum filtration/storage vial system (Corning, USA) was used to remove large non-exosomal particles, including cells, cellular debris, microvesicles and apoptotic vesicles. Then, a 300 kDa molecular weight filter was used to dilute the primary exosome filtrate to 50 mL via tangential flow filtration (Repligen, Cambridge, MA). A qEV10 size exclusion chromatography column (Izon, USA) was selected for the fine purification of exosomes, and a 0.22 μm filter was used to elute the exosomes with D-PBS. Finally, 5 mL of the eluate was collected for subsequent experiments. This approach is instrumental in reducing cell culture contaminants with a high rate of EV recovery.[12]

MSC-EV Protein Analysis by ExoView®

To analyze EV markers without contaminants, we utilized the new single-particle interferometric reflectance imaging sensor (SP-IRIS) ExoView® R200 (now Leprechaun from Unchained Labs, Pleasanton, CA, USA), which can measure the EV phenotype and biomarker colocalization. This technology is based on the single-particle interferometric reflectance imaging technique, which has been used to detect viruses and EVs as small as 50 nm in size.[13] The procedures followed the manufacturers' protocol. Capture anti-bodies against the positive markers CD63, CD81, and CD9 together with the negative control MIgG were selected on SP-IRIS silicon chips. The immobilization density of the antibody probes could be quantified by IRIS images and software.

Nanoparticle Tracking Analysis (NTA)

Nanosight NS300 (Malvern Panalytical, British) was used to analyze suspensions containing MSC-EVs. The procedures followed the manufacturers' protocol. NTA software was used to analyze the MSC-EV samples, which were optimized to first identify and then track the particles on a frame-by-frame basis, after which Brownian movement was tracked and measured from frame to frame. The particle size was determined by applying the two-dimensional Stokes–Einstein equation in terms of the velocity of particle movement. In this study, NTA was used to measure the nanoparticles in unlabeled MSC-EVs, PKH26 labeled MSC-EVs, PKH67 labeled MSC-EVs, ultracentrifuged PKH26 dyes and ultracentrifuged PKH67 dyes.

Transmission Electron Microscopy (TEM)

MSC-EVs were diluted 1:10 in distilled water. Ten microliters were loaded on a carbon-coated copper grid for 1 min, and the excess sample suspension was blotted with filter paper. The grid was placed on a drop of 1% phosphotungstic acid solution in Milli-Q ® water for 1 min. The excess stain was removed. The morphology of the EVs was examined by TEM.

Protein Quantification

The protein content of all the isolated MSC-EV samples was measured using a bicinchoninic acid (BCA) protein assay (Beyotime, Shanghai, China) according to the manufacturer's instructions. Briefly, each sample (20 μL) was mixed with a working reagent (200 μL, 50:1 ratio of assay reagents A to B) in a 96-well plate, which was then incubated for 20–30 min at 37 °C. After cooling to room temperature, sample absorbance was measured using a spectrophotometer (BioTek Multi-Mode Microplate Reader) at 562 nm and converted to protein concentration via a standard curve.

PKH Labeling of MSC-EVs

EVs isolated from MSCs were labeled with PKH26 (red fluorescent cell linker kit MINI26; Sigma–Aldrich Co., USA) or PKH67 (green fluorescent cell linker kit MINI67; Sigma–Aldrich Co., USA) according to the manufacturer's instructions. Briefly, the MSC-EVs were first resuspended in Diluent C (500 μL), after which 2 μL of PKH26 or PKH67 dye was added to Diluent C (500 μL) and mixed with the MSC-EV solution for 5 min of incubation in the dark. Subsequently, 1 mL of 1% BSA was added to stop the staining for at least 1 min. The unincorporated dyes were removed by 2 times EV centrifugation at 100,000×g for 70 min at 4 °C using an Eppendorf CP-90NX ultracentrifuge (Himac, Japan). EVs were washed with PBS and subjected to additional centrifugation. Then, the pellet was resuspended in PBS for further use. PKH26 dyes alone or PKH67 dyes alone without MSC-EVs were conducted 2 times ultracentrifuge with the same procedures as controls to validate the clearance of free PKH dyes or nanoparticles formed by PKH dyes.

Animals

Adult male C57BL/6J mice weighing 20–24 g were purchased from Charles River Laboratories (Beijing, China). Animals were housed in the animal facility at the Institute of Translational Medicine of the First Hospital of Jilin University. Mice were housed in an environmentally controlled room with a 12:12-h light and dark cycle and were given food and water ad libitum. The ethical committee of the first hospital of Jilin University approved this study. All experiments were performed following guidelines and regulations of the ethical committee of the first hospital of Jilin University.

Delivery of MSC-EVs

The intravenous route of MSC-EV administration was conducted via tail vein injection assisted by a tail vein injection assistance machine, and the intraperitoneal route of MSC-EV administration was conducted via intraperitoneal injection. One hundred micrograms of PKH26-labeled MSC-EVs in 200ul PBS were administered by the intravenous route, and 100 μg of PKH67-labeled MSC-EVs in 200ul PBS were administered by the intraperitoneal route simultaneously in one mouse. After 1 h, 6 h, 12 h and 24 h, the mice were anesthetized with 4% chloral hydrate (400 mg/kg, i.p) and transcardially perfused with PBS followed by perfusion with 4% PFA (both 10 mL/min, 100 mL). Immediately, the brains were dissected, immersed in 4% PFA (pH 7.4) for at least 2 h at room temperature, and stored at 4 °C. Coronal brain sections (30 μm thick) were obtained using a vibratome (Leica, Wetzlar, Germany) at approximately +0.98 to −0.46 mm from bregma (corpus striatum level) (Figure 1A). The brain slices were fixed and incubated for at least 10 min with fluoro-adsorbed DAPI (Sigma–Aldrich). Each group contained at least 6 mice.

Confocal Microscopy

Slice images for MSC-EV observation were acquired using an 8-bit grayscale confocal laser scanning microscope (Olympus FV1000). Approximately 3–6 0.7 μm thick confocal sections were captured parallel to the coverslip (XY sections), at the motor cortex (M), somatosensory cortex (S) and caudoputamen (CP) using a ×20 objective and ×100 oil immersion objective, respectively (Figure 1A). Z-stack reconstructions were generated with a thickness of 20 μm.

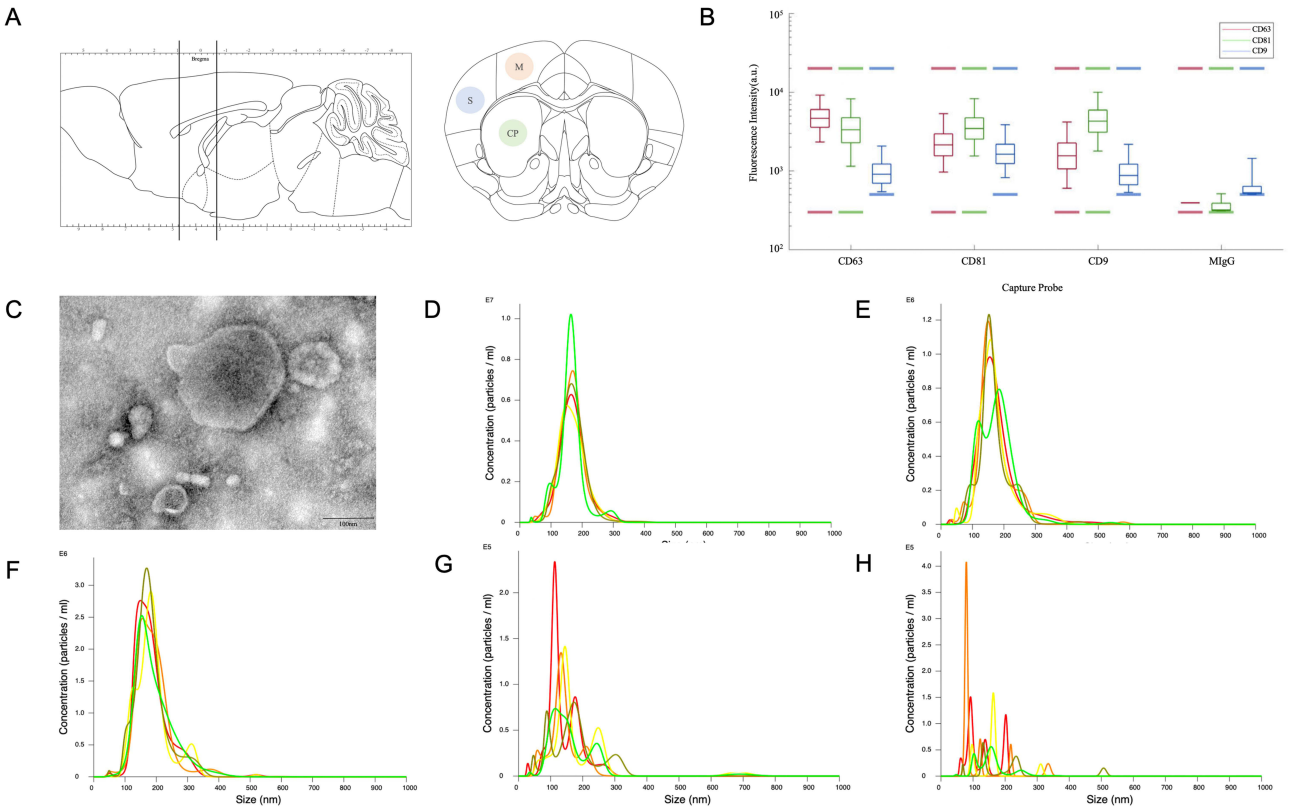

Figure 1 (**A**) Sketch of the coronal slicing range and captured sections of the motor cortex (M), somatosensory cortex (S) and caudoputamen (CP). (**B** and **C**) The results of protein analysis by ExoView® and transmission electron microscopy. (**D–H**) The results of NTA of unlabeled MSC-EVs, PKH26 labeled MSC-EVs, PKH67 labeled MSC-EVs, PKH26 dyes after the same ultracentrifugation procedures and PKH67 dyes after the same ultracentrifugation procedures.

Statistical Analysis

Statistical analyses were carried out using GraphPad Prism (version 10.2.0) software. One-way analyses of variance (ANOVA) were used to assess significance. Data in the text are presented as means ± SEM, and all analyses considered a value of $P \leq 0.05$ to be statistically significant.

Results

MSC-EV Characterization

Figure 1B-H show the MSC-EVs used in this study, which were characterized by TEM, NTA and ExoView® protein analysis. ExoView® protein analysis revealed that MSC-EVs expressed the EV markers CD63, CD81, and CD9, while the negative marker MIgG was barely expressed (Figure 1B). TEM demonstrated that the MSC-EVs were small vesicles, most of which were less than 200 nm in size (Figure 1C). The NTA analysis showed that the average diameter of the unlabeled MSC-EVs, PKH26 labeled MSC-EVs, PKH67 labeled MSC-EVs, ultracentrifuged PKH26 dyes without MSC-EVs and ultracentrifuged PKH67 dyes without MSC-EVs were 153.9 nm, 164.8nm, 169.9nm, 115.7nm and 79.3nm (Figure 1D-H). The particle number of ultracentrifuged PKH dyes without MSC-EVs was at least more than 100 times smaller than the concentration of PKH labeled MSC-EVs. The particle to protein ratio was about 2.388E+8 particles/ug.

Brain and Liver Distribution of PKH-Labeled MSC-EVs Observed by Confocal Microscopy Using a ×20 Objective

Using a ×20 objective, we could observe only uniform background fluorescence in the PKH26 or PKH67 fluorescence channels without any specific PKH26- or PKH67-labeled MSC-EVs in any brain section after 1 h, 6 h, 12 h or 1 day of 100 μg of PKH-labeled MSC-EV administration (Figure 2A-C). However, using a ×20 objective is feasible for observing

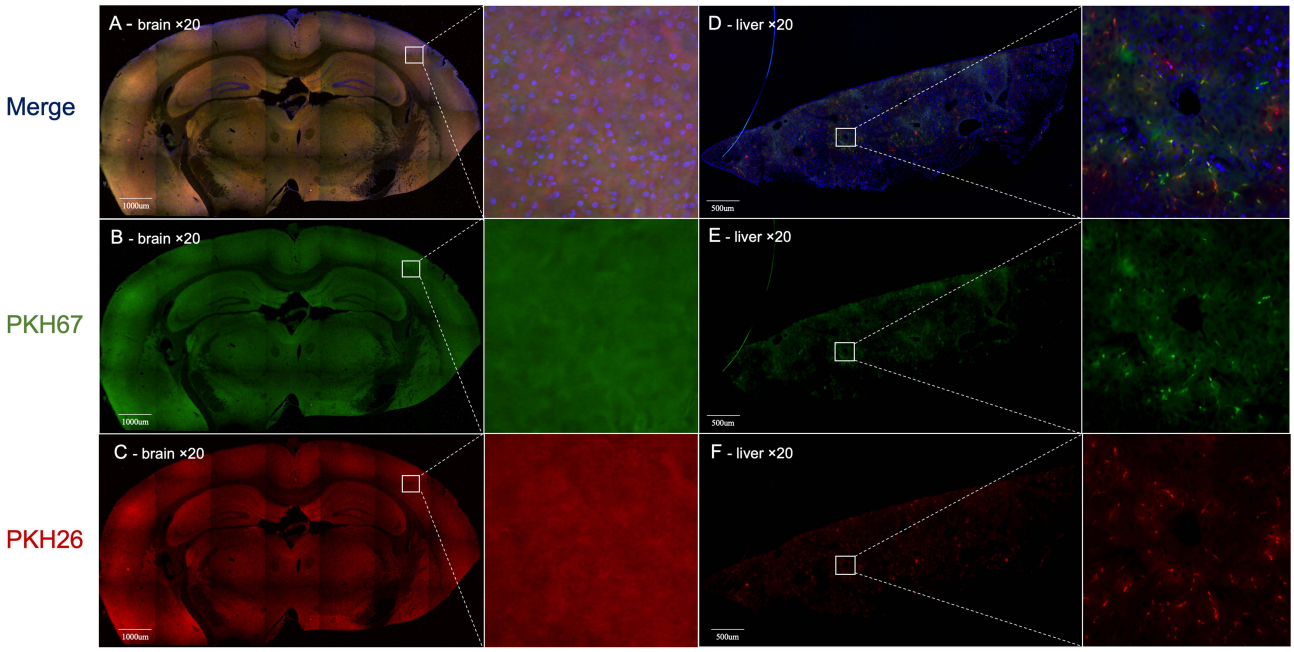

Figure 2 (**A - C**) Images of the brain obtained by using ×20 objective confocal microscopy. Only uniform background fluorescence in the PKH26 or PKH67 fluorescence channels was observed without any specific PKH26- or PKH67-labeled MSC-EVs in any brain section. (**D-F**) Liver analysis by using ×20 objective confocal microscopy. Both the PKH26 and PKH67 fluorescence channels showed obvious fluorescence, which had the same position distribution and different distributions in liver slices. Blue: DAPI; Green: PKH67 fluorescence channel; Red: PKH26 fluorescence channel. The white line square shows the position of the amplified picture.

the distribution of 100 μg of PKH26- and PKH67-labeled MSC-EVs in the liver. Both the PKH26 and PKH67 fluorescence signals exhibited the same position distribution and different position distributions in liver slices, demonstrating that MSC-EVs administered via the intravenous or intraperitoneal route exhibited different distributions in the liver (Figure 2D-F).

Brain and Liver Distribution of PKH-Labeled MSC-EVs Observed by Confocal Microscopy Using a 100× Oil Immersion Objective

Then, we used a ×100 oil immersion objective to observe PKH-labeled MSC-EVs in the brain and liver. As a result, we detected dotted fluorescence in both the PKH26 and PKH67 fluorescence channels in brain slices, which might indicate PKH26- or PKH67-labeled MSC-EVs in the M, S and CP zones. However, PKH26 fluorescence and PKH67 fluorescence had identical distributions at all observation positions (Figure 3). In addition, we observed a similar distribution of PKH-labeled MSC-EVs in the liver compared with the results obtained using a ×20 objective. Both the PKH26 and PKH67 fluorescence signals exhibited the same position distribution and different position distributions in liver slices (Figure 4A and B). Then, brain slices without PKH-labeled EVs were observed, and the distribution of the PKH26 and PKH67 fluorescence was similar to that of PKH-labeled EVs (Figure 4C and D).

PKH26- and PKH67-Labeled MSC-EVs in PBS In vitro, Brain and Liver Distribution of MSC-EVs Labeled with 1000 μg of PKH67 Observed by Confocal Microscopy

After PKH26 and PKH67 labeling, two kinds of MSC-EVs mixed in PBS were dropped on glass slides, covered with coverslips, and directly observed by confocal microscopy. Both the PKH26- and PKH67-labeled MSC-EVs were small dots with obvious fluorescence. All the dotted PKH26 and PKH67 fluorescence signals appeared at different positions without any identical distribution (Figure 5A). Then, we increased the amount of PKH67-labeled MSC-EVs to 1000 μg and administered them to mice through intravenous injection. Confocal microscopy of brain slices revealed similar results of brain observation compared with those of the 100 μg injection and control groups. No specific fluorescence was detected using a ×20 objective in brain slices, and an identical distribution of PKH26 and PKH67 fluorescence was detected using a ×100 oil immersion

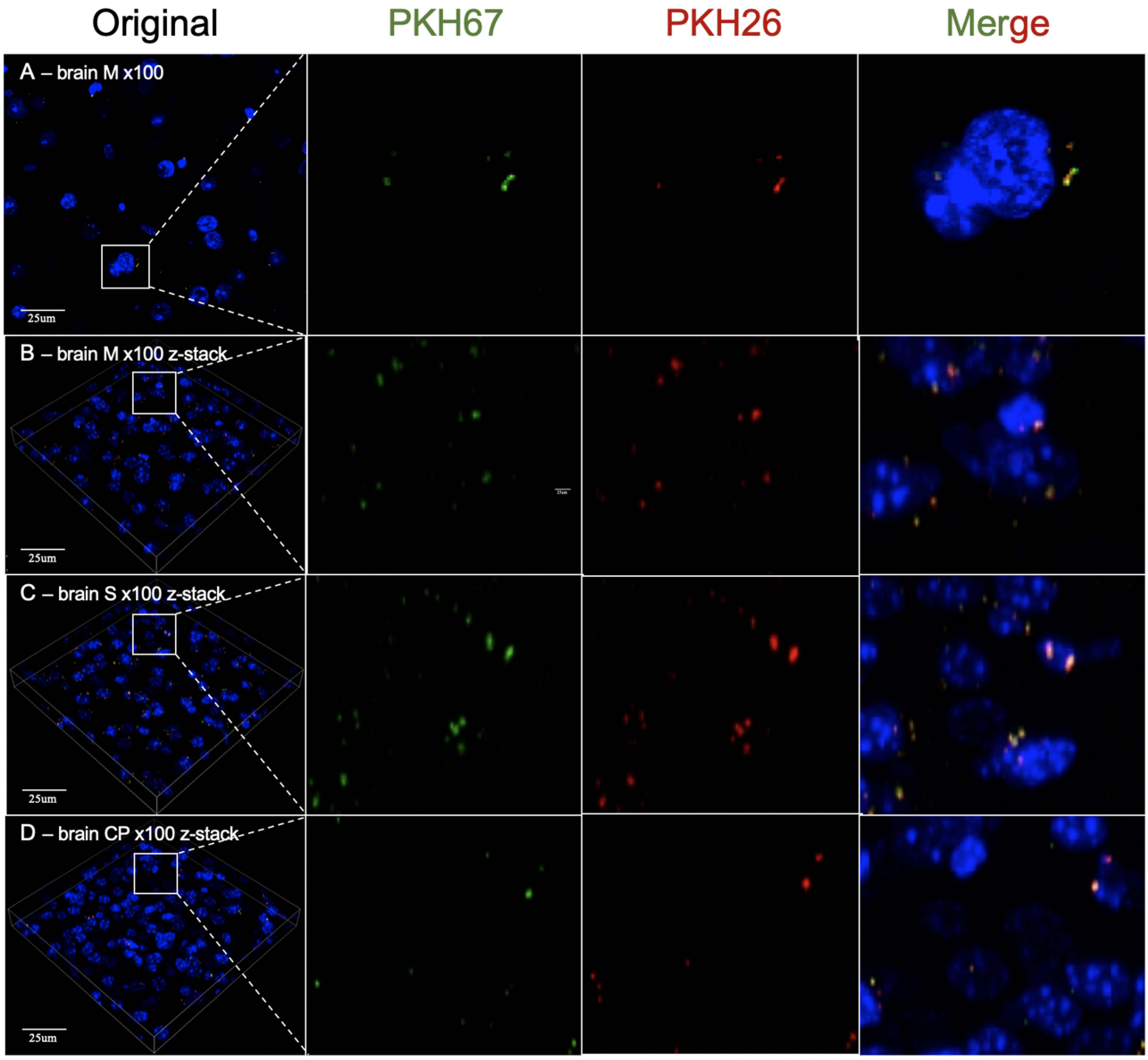

Figure 3 (**A**) 2D images of the motor cortex (M) of the brain obtained by using ×100 oil immersion objective confocal microscopy. (**B**) The z-stack reconstruction image of the motor cortex (M) of the brain obtained by using ×100 oil immersion objective confocal microscopy. (**C**) The z-stack reconstruction image of the somatosensory cortex (S) of the brain obtained by using ×100 oil immersion objective confocal microscopy. (**D**) Images of the z-stack reconstructed at the caudoputamen (CP) of the brain obtained by using ×100 oil immersion objective confocal microscopy. Blue: DAPI; Green: PKH67 fluorescence channel; Red: PKH26 fluorescence channel. The white line square shows the position of the amplified picture.

objective even when PKH26-labeled MSC-EVs were not administered (Figure 5B–D). The intensity and density of PKH67 fluorescence in the liver slices from the 1000 μg PKH67-labeled MSC-EV group were obviously greater than those in the liver slices from the 100 μg injection group according to the ×20 objective and ×100 oil immersion objective (Figure 6A–C).

Quantification of PKH26 and PKH67 Fluorescent Puncta in Different Brain Regions and Different Groups

The number of PKH26 and PKH67 fluorescent puncta per x100 vision in motor cortex, somatosensory cortex and caudoputamen was counted in the group with 100 ug PKH26 labeled MSC-EVs and 100 ug PKH67 labeled MSC-EVs administered through intravenous route and intraperitoneal route respectively and simultaneously. The quantification did not reveal statistically significant difference between different brain regions (Figure 7A). Similar findings were obtained

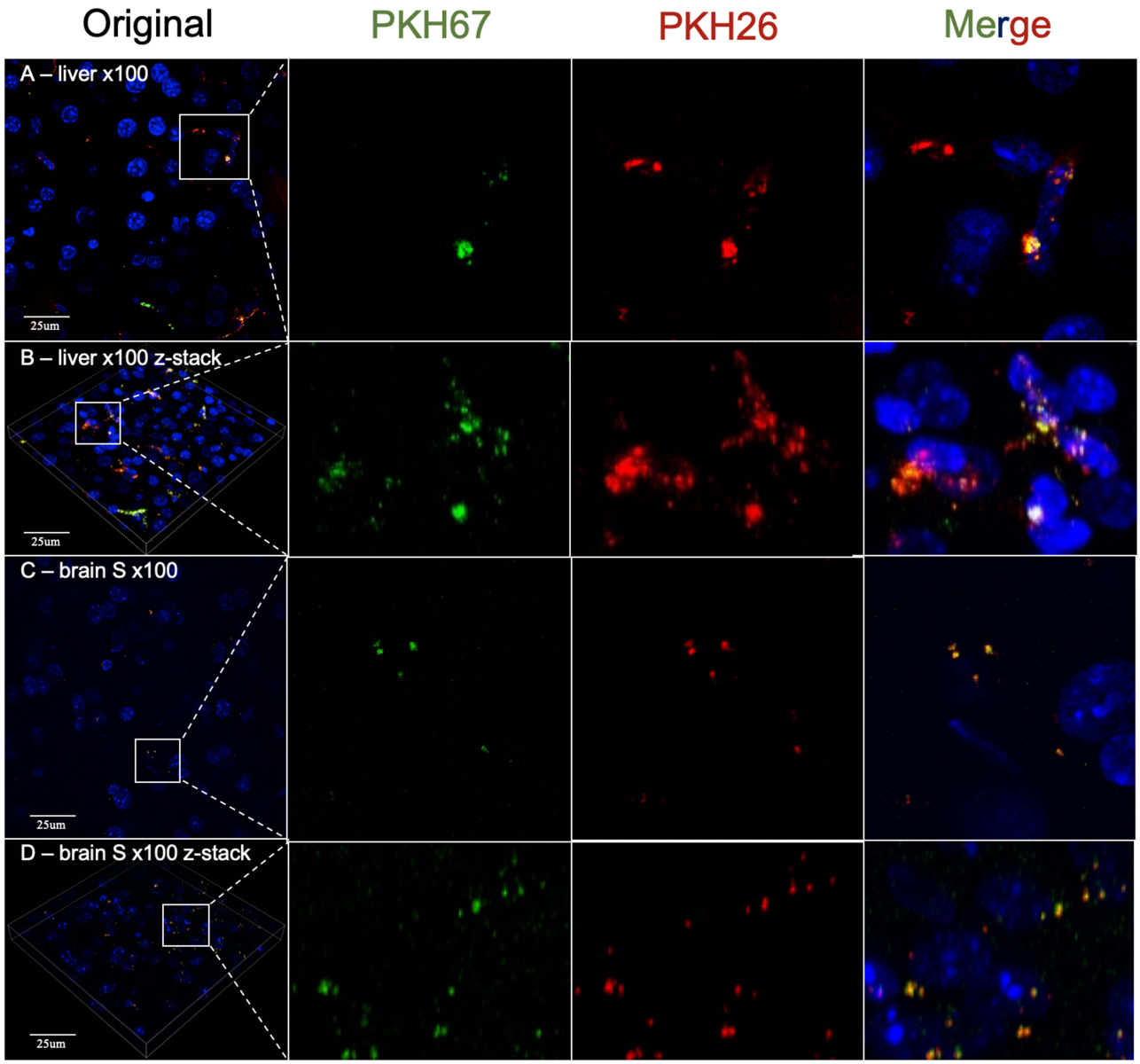

Figure 4 (**A**) 2D images of the liver obtained by using ×100 oil immersion objective confocal microscopy. (**B**) The z-stack reconstruction image of the liver obtained by using ×100 oil immersion objective confocal microscopy. (**C**) A 2D image of the somatosensory cortex (S) of the brain without PKH-labeled MSC-EVs was obtained via confocal microscopy with a ×100 oil immersion objective obtained by using ×100 oil immersion objective confocal microscopy. (**D**) Images of the z-stack reconstructed image of the somatosensory cortex (S) of the brain without PKH-labeled MSC-EVs obtained by using ×100 oil immersion objective confocal microscopy. Blue: DAPI; Green: PKH67 fluorescence channel; Red: PKH26 fluorescence channel. The white line square shows the position of the amplified picture.

when the number of fluorescent puncta were quantified in motor cortex of the control group, PKH26 and PKH67 labeling EVs administration group and tenfold PKH67 administration group (Figure 7B). No statistically significant difference was found.

Discussion

The therapeutic effect and drug transportation capacity of EVs have been utilized for the treatment of neurological disorders. EVs isolated from MSCs, neurons and inflammatory cells have a high penetration rate through the BBB.[14] Many studies have proven the therapeutic efficacy of EVs.[1,6,7,15] PKH dyes are lipophilic long-chain carbocyanine dyes commonly used to stain EVs for distribution studies.[10] In vivo visualization of intravenously injected PKH67-labeled EVs via an in vivo imaging system (IVIS; Kodak, Rochester, NY, USA) has been studied.[16] In vivo imaging of live mice

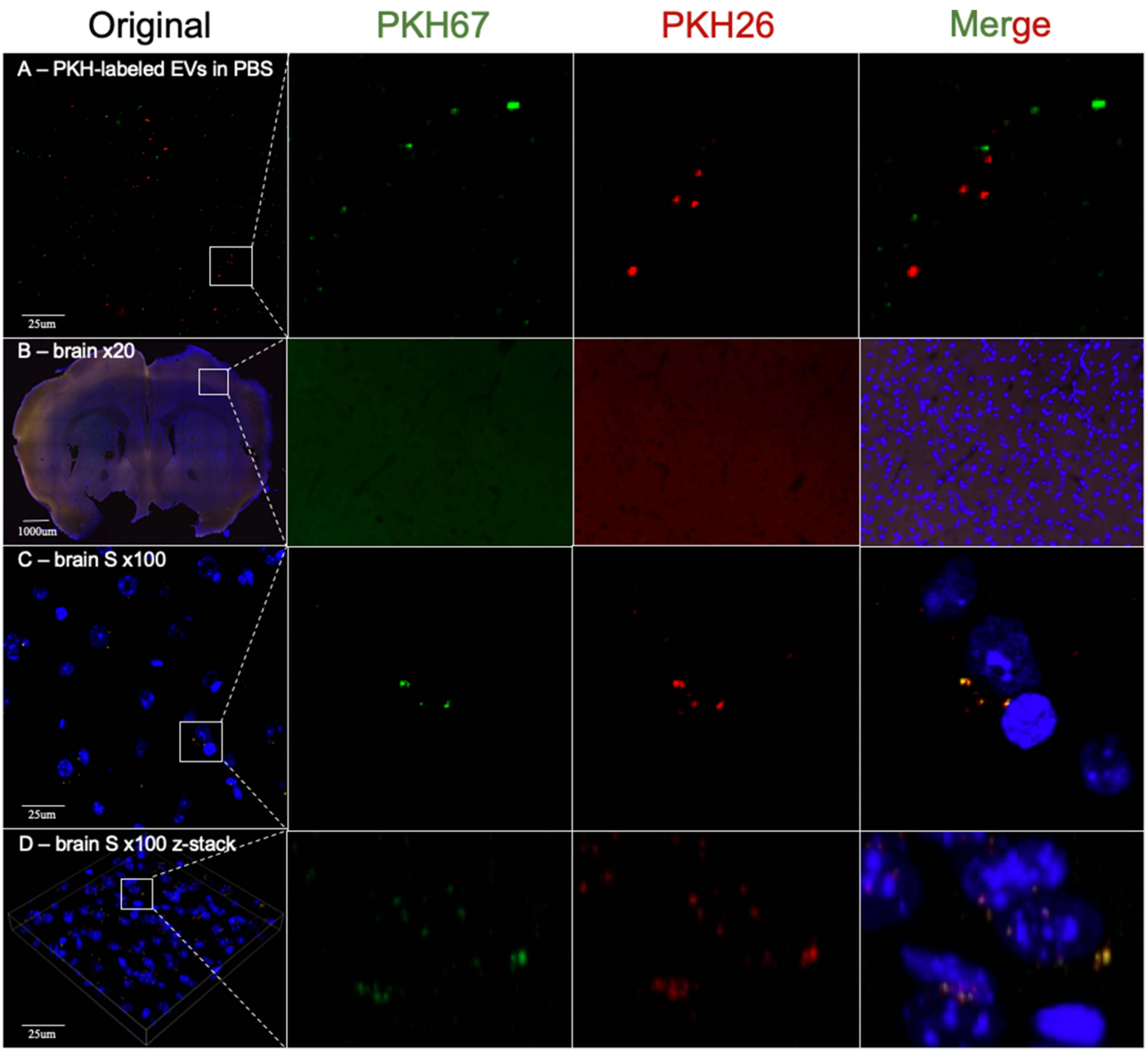

Figure 5 (**A**) Image of mixed PKH26- and PKH67-labeled MSC-EVs in PBS obtained by using ×100 oil immersion objective confocal microscopy. (**B**) Image of the brain after administration of 1000 μg of PKH67-labeled MSC-EVs by using ×20 objective confocal microscopy. (**C** and **D**) 2D and z-stack reconstruction images of the somatosensory cortex (S) of the brain after administration of 1000 μg of PKH67-labeled MSC-EVs obtained by using ×100 oil immersion objective confocal microscopy. Blue: DAPI; Green: PKH67 fluorescence channel; Red: PKH26 fluorescence channel. The white line square shows the position of the amplified picture.

after intravenous administration of PKH67-labeled EVs demonstrated that compared with those in the liver, lung, spleen and kidney, only a few EVs were distributed in the brain. However, multiple studies have applied PKH dyes to demonstrate the presence of EVs in the brain after intravenous, intraperitoneal or intranasal injection.[17–21] A schematic figure of this study was shown in Figure 8. The initial aim of this study was to explore the probable differences in the distributions of intravenously and intraperitoneally administered EVs in the brain. Different administration routes are known to have different body biodistributions, and different EV target organs need to use the most appropriate administration routes for treatment.[11] We administered PKH26-labeled MSC-EVs through the intravenous route and PKH67-labeled MSC-EVs through the intraperitoneal route simultaneously in the same mouse. Then, the MSC-EV distribution was observed by confocal microscopy. Accidentally, identical fluorescence positions of the PKH26 and PKH67 fluorescence channels were detected in brain coronal slices, while the distributions of the two kinds of fluorescence were more complicated in the liver. This result prompted us to investigate the imaging characteristics of

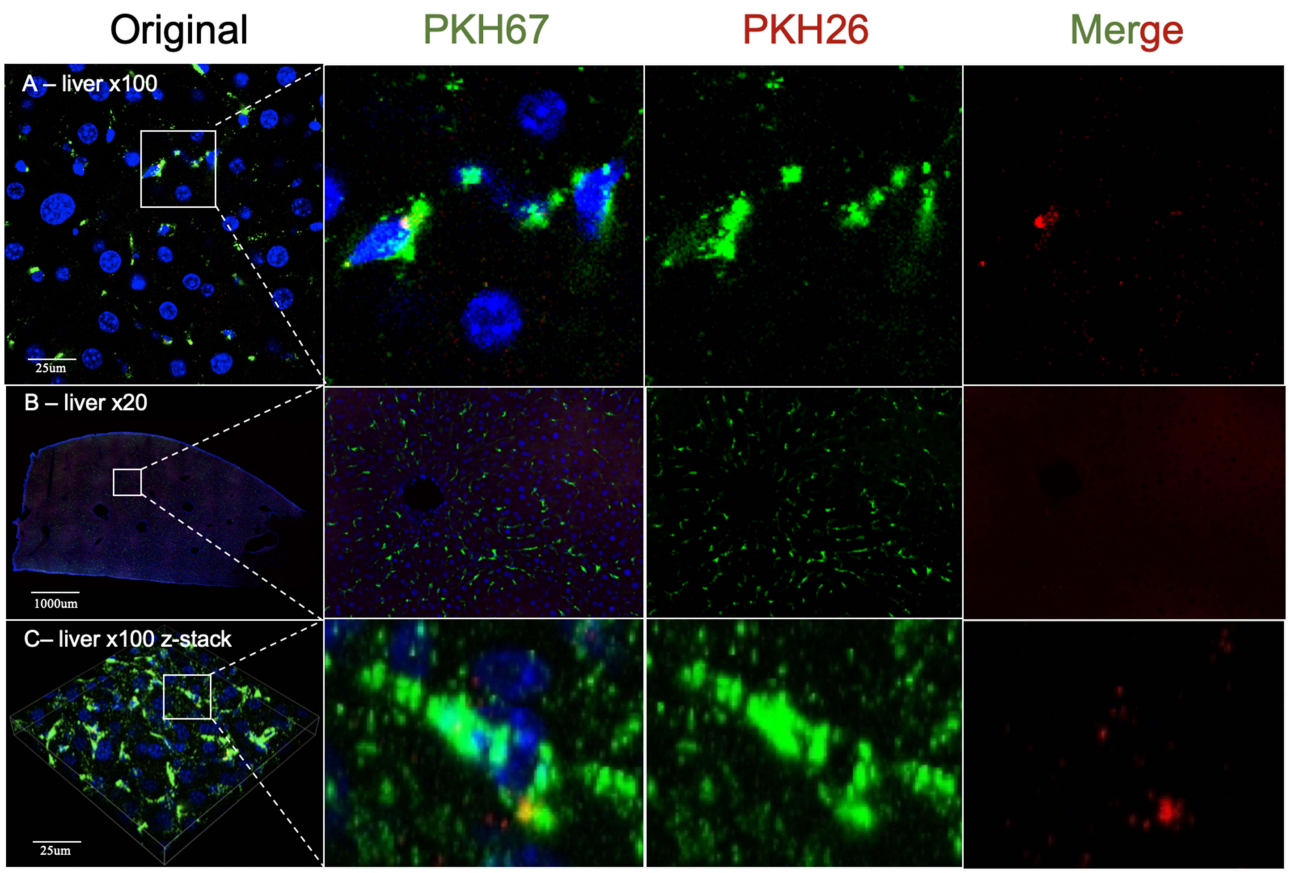

Figure 6 (**A**) A 2D image of the liver after administration of 1000 μg of PKH67-labeled MSC-EVs by using ×100 oil immersion objective confocal microscopy. (**B**) Image of the liver treated with 1000 μg of PKH67-labeled MSC-EVs obtained via ×20 objective confocal microscopy. (**C**) A z-stack reconstruction image of the liver after administration of 1000 μg of PKH67-labeled MSC-EVs obtained by using ×100 oil immersion objective confocal microscopy. Blue: DAPI; Green: PKH67 fluorescence channel; Red: PKH26 fluorescence channel. The white line square shows the position of the amplified picture.

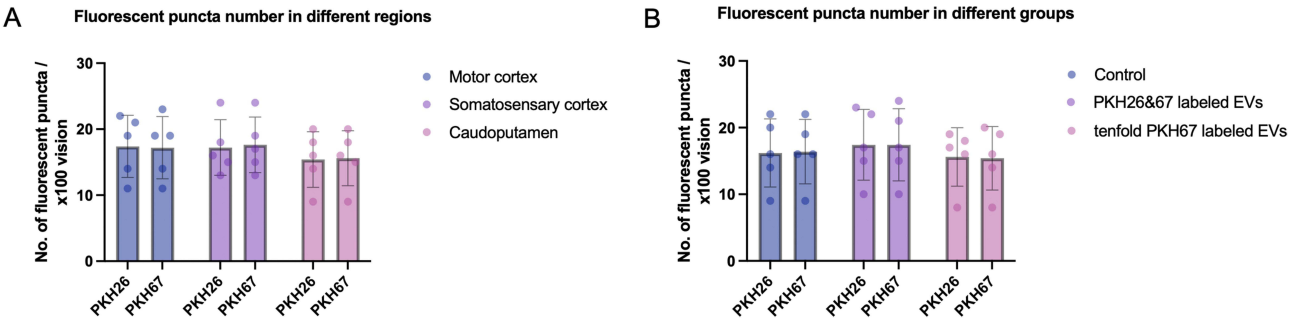

Figure 7 (**A**) Quantification of PKH26 and PKH67 fluorescent puncta per x100 vision in motor cortex, somatosensory cortex and caudoputamen in the group with 100 ug PKH26 labeled MSC-EVs and 100 ug PKH67 labeled MSC-EVs administered through intravenous route and intraperitoneal route respectively and simultaneously. Differences between brain regions were not found to be statistically different. (**B**) Quantification of PKH26 and PKH67 fluorescent puncta per x100 vision in the motor cortex of the control group, PKH26 and PKH67 labeling EVs administration group and tenfold PKH67 administration group. Differences between groups were not found to be statistically different.

PKH-labeled EVs in the brain through confocal microscopy. Since studies have applied PKH dyes to demonstrate the presence of EVs in the brain, no systematic study of the imaging characteristics of PKH-labeled EVs in the brain through confocal microscopy has been conducted.

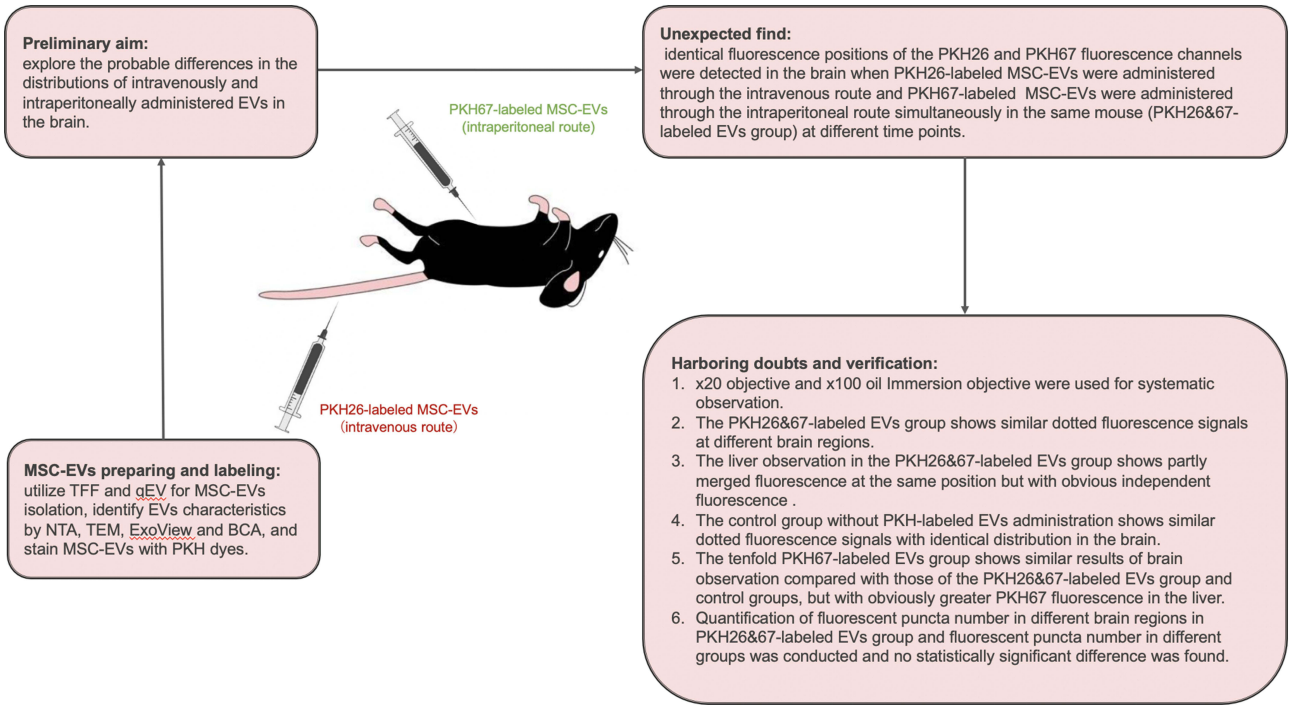

Figure 8 A schematic figure of the study.

First, we used a ×20 objective to observe the distribution of PKH-labeled dyes in the brain. However, only uniform background fluorescence in the PKH26 or PKH67 fluorescence channels was observed, and no specific PKH26- or PKH67-labeled MSC-EVs were detected in any brain area after the administration of 100 μg of PKH-labeled MSC-EVs for 1 h, 6 h, 12 h or 1 day. However, in the liver, the distribution of PKH-labeled MSC-EVs was successfully observed using a ×20 objective (Figure 2). We assume that the negative results for the brain might be attributed to the small amount of EVs that are able to cross the brain through the BBB and the small size and low fluorescence of EVs. Almost all studies using PKH dyes to identify EVs in the brain have shown EVs at ×100 magnification.[17–21] Therefore, we further observed the slices using a 100× oil immersion objective. Dotted fluorescence signals were observed in both the PKH26 and PKH67 fluorescence channels, which are thought to represent the presence of intravenous and intraperitoneal MSC-EVs when we use a relatively high laser intensity and adjust LUTs to a relatively small range. However, the two kinds of dotted fluorescence signals were identical in the brain coronal slices (Figure 3). There was no difference in the distribution of MSC-EVs at different time points. We know that the intravenous and intraperitoneal routes of EV absorption are different. The distribution of EVs administered by the two routes should not be completely the same in the brain. The liver observation results further confirmed that the two kinds of fluorescence signals were partly merged at the same position with independent fluorescent dots, which indicates the difference between the two administration routes (Figure 4A and B). It is recognized that mitochondria, collagen and lipofuscin can give off autofluorescence.[22] Cerebral autofluorescence is highly abundant of lipofuscin and is often particularly strong in structures of the same size and brightness as nanoparticles. Some researchers have found that neurons and endothelial cells can have strong auto-fluorescence.[23] Thus, we doubted that the dotted fluorescence signals in the brain were PKH-labeled MSC-EVs or only background fluorescence. This assumption contradicts previous observations of PKH-labeled EVs in the brain by confocal microscopy.[17–21] However, only this study simultaneously observed the fluorescence signals of PKH26- and PKH67-labeled EVs in the same sample, while other studies used only one kind of PKH dye to determine the distribution of EVs in the brain. Compared with those in the PKH-labeled MSC-EV group, the dotted fluorescence signals in the control group without PKH-labeled MSC-EVs were similar (Figure 4C and D). Mixed PKH26- and PKH67-labeled MSC-EVs in PBS were directly observed by confocal microscopy, and the results showed that PKH26- and PKH67-labeled MSC-EVs were both small dots with obvious fluorescence at a lower laser intensity and a larger LUT range than

those observed in brain slices. No position coincidence of the two fluorescence signals was observed, indicating that PKH26 and PKH67 normally cannot mutually influence the fluorescence in each emission spectrum (Figure 5A). As a result, the dotted fluorescence signals we detected in brain slices by confocal microscopy might be auto-fluorescence. Therefore, no MSC-EVs were observed in brain slices. We further increased the amount of PKH-labeled MSC-EVs from 100 μg to 1000 μg to better observe the distribution of the MSC-EVs in the brain. However, after 1000 μg of PKH67-labeled MSC-EVs were administered through the tail vein, the brain slices exhibited the same changes in the PKH26 and PKH67 fluorescence signals (Figure 5B and C), while the liver slices exhibited more PKH67 fluorescence signals and fewer auto PKH26 channel fluorescence signals than did the 100 μg MSC-EVs (Figure 6). Furthermore, the quantification of fluorescent puncta number in different brain regions and different groups was conducted and reveal no statistically significant difference between different brain regions and groups (Figure 7).

It is reported that PKH-labeled EVs can be contaminated by non-EV particles formed by PKH dyes during the PKH labeling procedure.[24] To verify the effectiveness of PKH dyes removing and the contamination of non-EV particles formed by PKH dyes, we used NTA to analyze PKH labeled MSC-EVs with 100-fold dilution and PKH dyes after the same ultracentrifugation procedures without dilution. The results showed that non-EV particles were formed by the PKH dyes. However, the particle number of non-EVs particles in PKH dyes after the same ultracentrifugation procedures was at least more than 100 times smaller than the particle number of PKH labeled MSC-EVs, which means that particles that would influence the accuracy of results were less than 1% of particles in PKH labeled MSC-EVs solution. For more information, we administered PKH26 dyes after the same ultracentrifugation procedures by intravenous route and PKH67 dyes after the same ultracentrifugation procedures by intraperitoneal route simultaneously in the same mouse to verify the influence of non-EV particles formed by PKH dyes after labeling and 2 times ultracentrifugation on the observation by confocal microscopy. Furthermore, we also administered original PKH26 solution by intravenous route and original PKH26 solution by intraperitoneal route simultaneously in the same mouse to verify the influence of probably existent free PKH dyes on the observation by confocal microscopy. The doses of PKH26 and PKH67 were identical to the doses we used in the procedures of MSC-EVs labeling. The result of the administration of PKH dyes after the same ultracentrifugation procedures is shown in Figure S1. Identical distributed dotted fluorescence signals of PKH26 and PKH67 channels were observed in both brain and liver, which might be auto-fluorescence. Therefore, non-EV particles formed by PKH dyes after the labeling procedure and 2 times ultracentrifugation have little influence on the observation of MSC-EVs biodistribution by confocal microscopy. The result of the administration of free PKH dyes is shown in Figure S2. Identical distributed dotted fluorescence signals of PKH26 and PKH67 channels were observed in the brain, similar to the results of control groups and groups with PKH labeled MSC-EVs administration. The fluorescence of PKH26 and PKH67 in the liver was patchy in distribution. Interestingly, PKH26 has obviously more distribution than PKH67 in the liver. We speculate that a portion of PKH67 dyes stayed in the peritoneal cavity. Thus, probably existent free PKH dyes have little influence on the observation of MSC-EVs biodistribution in the brain by confocal microscopy.

In view of the above, the authenticity of the fluorescence signals representing the MSC-EVs we observed in brain slices via confocal microscopy is unclear. It is worth noting whether these fluorescence signals are just background fluorescence. Some researchers also question the effectiveness of using PKH dyes to stain EVs for distribution studies and believe that imaging of EVs after PKH labeling can only reveal large aggregates of EVs, but such large aggregates are unlikely to occur in the brain via venous or peritoneal routes.[7] Kang et al undertook a systematic review of the literature to summarize the biodistribution of EVs following administration into animals.[7] 38 studies were included in their study. EVs biodistribution was investigated in a total of 20 different organs in recipient rodents. The brain uptake of EVs was commonly studied, which was reported in 26 studies. Compared to the abundant aggregation of EVs in liver, lung, spleen and kidney, the brain showed low or no localization of EVs within 24 hours. The information on brain localization after 24 hours was insufficient in the literature. Thus, it has been recognized that only a small number of EVs (less than 1%) can cross the blood-brain barrier and enter the brain in rodents.[7,8] For the biodistribution of EVs in non-human primate model, Driedonks et al investigated the pharmacokinetics and biodistribution of EVs labeled with a highly sensitive nanoluciferase reporter (palmGRET) in a non-human primate model (Macaca nemestrina) and mice, comparing intravenous and intranasal administration.[22] The results also show that the brain uptake of EVs was negligible whether EVs were given through intravenous or intranasal approach in both animals. EVs administered by intravenous

injection were most efficiently taken up by the liver in accordance with many other EV biodistribution studies.[7–9,11] Interestingly, signals of labeled EVs could be observed in cerebrospinal fluid (CSF) after intravenous administration at high doses and remained detectable above the background for up to 24 hours. However, signals of labeled EVs were not detectable in the brain after intrathecal injection. Therefore, blood-brain or CSF-brain routes are neither a superhighway for EVs entering the brain.

We evaluated studies in which PKH-labeled EVs distributed in the brain were observed by confocal microscopy. The results of single PKH dye staining, which revealed PKH-labeled EVs as small dotted fluorescence signals at ×100 magnification via confocal microscopy, are similar to our observations of MSC-EVs. Zhuang et al isolated EVs from MSCs for the treatment of traumatic brain injury.[17] They found that EVs isolated from MSCs could attenuate neurological damage in traumatic brain injury by alleviating glutamate-mediated excitotoxicity. PKH67 was used to label EVs, and 100 μg of PKH67 was administered through the tail vein. After 24 h, brain slices were incubated with GFAP antibodies to study the colocalization of EVs with astrocytes in the cortex. According to their confocal microscopy images (Figure S3), EVs are also small green dots at ×100 magnification, which is similar to our results. There is no counterpart at the same position in the red fluorescence. However, this might be attributed to the strong fluorescence from GFAP staining, which can be observed at low laser intensities, preventing background fluorescence. Dabrowska et al reported that MSC-EVs could attenuate inflammation induced by ouabain in the focal brain injury.[20] PKH26 was used to label EVs, and 1.3×10 9 EVs were administered through the internal carotid artery. After 24 h, the brain slices were observed by confocal microscopy. The images of the EVs also showed small red dots at 100× magnification, which is similar to our results (Figure S4). These small red dots are difficult to distinguish from background fluorescence. Ioannides et al administered 6.70×10 6 PKH26-labeled EVs isolated from human neural stem cells via three distinct routes—intrahippocampal transplantation, retro-orbital vein injection, and intranasal—to explore differences in the amount of EVs able to translocate across the brain.[18] The captured images showed that the EVs in the prefrontal cortex, subventricular zone and hippocampus were also small red dots at 100× magnification (Figure S5 and S6). There was no significant difference in the quantification of EVs throughout the brain (Figure S7). The authors concluded that three administration routes afforded effective penetrance and perfusion of EVs throughout the brain and that the functional equivalence of each administration route effectively delivered EVs to the brain parenchyma.[18] However, from our perspective, this functional equivalence of each administration route indicates that the fluorescent dots observed by confocal microscopy might be background fluorescence rather than PKH-labeled EVs. However, their study did not include data from a group that received no PKH-labeled EVs. Kodali et al conducted a study to determine whether brain injury-induced signals are essential for the entry of administered EVs into different brain regions.[19] They administered 1×10 10 PKH26-labeled EVs isolated from MSCs. After 6 h, PKH26-labeled EVs were quantified from multiple forebrain regions using serial brain sections processed for different neural cell markers and confocal microscopy. The captured images show that the EVs are also small red dots at ×100 magnification. In both intact and status epilepticus-injured forebrains, EVs are “delivered” into neurons and microglia. To confirm that the PKH26-positive particles found inside neurons are EVs, they also processed brain tissue sections for NeuN and CD63 dual immuno-fluorescence staining and examined the co-expression of CD63 with PKH26-positive particles. The results showed that PKH26 red fluorescence and CD63 green fluorescence mostly occurred at the same location (Figure S8). The authors believe that this result indicates the authentication of EVs detected in brain tissue. However, there is a doubt that no independent green dots were found in the brain, which is inconceivable because there must be many more endogenous EVs that can be labeled by CD63 antibodies than PKH-labeled EVs in the brain.

Therefore, the small fluorescent dots observed by ×100 magnification confocal microscopy might not be specific PKH-labeled EVs but rather background fluorescence. It is doubted whether the use of PKH dyes to stain EVs is an appropriate approach for determining the distribution of EVs by confocal microscopy. In addition, some pitfalls associated with the use of PKH dyes for EV staining have been reported, including lipoprotein contamination in EV samples, the desorption of PKH dyes from vesicles into proteins and lipoproteins in blood and serum, and the ability of amphiphilic PKH dye compounds to form EV-like particles.[10,24,25] The latest MISEV guidelines referred to the caution against using these PHK-type dyes because of unreliable EV tracking, dye transfer, and poor quantification.[26] Thus, the

use of PKH dyes to study EV distribution in the brain might have produced conflicting results, and the use of PKH dyes in this kind of study should be prudent.

Conclusion

In summary, the results of this study provide a warning about the use of PKH dyes as a labeling method for EVs to study brain distribution via confocal microscopy. Only large aggregates of EVs labeled by PKH dyes inside the tissue can be visualized such as liver, but such large aggregates are unlikely to occur in the brain via venous or peritoneal routes. The autofluorescence of the tissue can be inferred by the observation of fluorescent signals in PKH26 and PKH67 fluorescence channels at the same time. Only a few fluorescent dots emerged independently, and they might have been PKH-labeled EVs. However, the brain distribution of EVs deduced from these few independent dots is unreliable.

Funding

The authors declare financial support was received for the research, authorship, and/or publication of this article. This study was supported by funding from the following: the education department of Jilin Province (JJKH20231210KJ) and Medical and Health Care Special Talents project of Jilin Province (JLSWSRCZX2021).

Disclosure

The authors report no conflicts of interest in this work.

References

1. Reed SL, Escayg A. Extracellular vesicles in the treatment of neurological disorders. *Neurobiol Dis*. 2021;157:105445. doi:10.1016/j.nbd.2021.105445
2. Hu Q, Zhang S, Yang Y, et al. Extracellular vesicles in the pathogenesis and treatment of acute lung injury. *Mil Med Res*. 2022;9(1):61. doi:10.1186/s40779-022-00417-9
3. Tang TT, Lv LL, Lan HY, Liu BC. Extracellular Vesicles: opportunities and Challenges for the Treatment of Renal Diseases. *Front Physiol*. 2019;10:226. doi:10.3389/fphys.2019.00226
4. Chulpanova DS, Kitaeva KV, James V, Rizvanov AA, Solovyeva VV. Therapeutic Prospects of Extracellular Vesicles in Cancer Treatment. *Front Immunol*. 2018;9:1534. doi:10.3389/fimmu.2018.01534
5. Fuhrmann G, Neuer AL, Herrmann IK. Extracellular vesicles - A promising avenue for the detection and treatment of infectious diseases? *Eur J Pharm Biopharm*. 2017;118:56–61. doi:10.1016/j.ejpb.2017.04.005
6. Saint-Pol J, Gosselet F, Duban-Deweer S, Pottiez G, Karamanos Y. Targeting and Crossing the Blood-Brain Barrier with Extracellular Vesicles. *Cells*. 2020;9(4). doi:10.3390/cells9040851
7. Kang M, Jordan V, Blenkiron C, Chamley LW. Biodistribution of extracellular vesicles following administration into animals: a systematic review. *J Extracell Vesicles*. 2021;10(8):e12085. doi:10.1002/jev2.12085
8. Nieland L, Mahjoum S, Grandell E, Breyne K, Breakefield XO. Engineered EVs designed to target diseases of the CNS. *J Control Release*. 2023;356:493–506. doi:10.1016/j.jconrel.2023.03.009
9. Yi YW, Lee JH, Kim SY, et al. Advances in Analysis of Biodistribution of Exosomes by Molecular Imaging. *Int J Mol Sci*. 2020;21(2):665. doi:10.3390/ijms21020665
10. Puzar Dominkus P, Stenovec M, Sitar S, et al. PKH26 labeling of extracellular vesicles: characterization and cellular internalization of contaminating PKH26 nanoparticles. *Biochim Biophys Acta Biomembr*. 2018;1860(6):1350–1361. doi:10.1016/j.bbamem.2018.03.013
11. Tolomeo AM, Zuccolotto G, Malvicini R, et al. Biodistribution of Intratracheal, Intranasal, and Intravenous Injections of Human Mesenchymal Stromal Cell-Derived Extracellular Vesicles in a Mouse Model for Drug Delivery Studies. *Pharmaceutics*. 2023;15(2). doi:10.3390/pharmaceutics15020548
12. Porzionato A, Zaramella P, Dedja A, et al. Intratracheal administration of clinical-grade mesenchymal stem cell-derived extracellular vesicles reduces lung injury in a rat model of bronchopulmonary dysplasia. *Am J Physiol Lung Cell Mol Physiol*. 2019;316(1):L6–L19. doi:10.1152/ajplung.00109.2018
13. Daaboul GG, Gagni P, Benussi L, et al. Digital Detection of Exosomes by Interferometric Imaging. *Sci Rep*. 2016;6:37246. doi:10.1038/srep37246
14. Rehman FU, Liu Y, Zheng M, Shi B. Exosomes based strategies for brain drug delivery. *Biomaterials*. 2023;293:121949. doi:10.1016/j.biomaterials.2022.121949
15. Niu X, Chen J, Gao J. Nanocarriers as a powerful vehicle to overcome blood-brain barrier in treating neurodegenerative diseases: focus on recent advances. *Asian J Pharm Sci*. 2019;14(5):480–496. doi:10.1016/j.ajps.2018.09.005
16. Naseri Z, Oskuee RK, Jaafari MR, Forouzandeh Moghadam M. Exosome-mediated delivery of functionally active miRNA-142-3p inhibitor reduces tumorigenicity of breast cancer in vitro and in vivo. *Int J Nanomed*. 2018;13:7727–7747. doi:10.2147/IJN.S182384
17. Zhuang Z, Liu M, Luo J, et al. Exosomes derived from bone marrow mesenchymal stem cells attenuate neurological damage in traumatic brain injury by alleviating glutamate-mediated excitotoxicity. *Exp Neurol*. 2022;357:114182. doi:10.1016/j.expneurol.2022.114182
18. Ioannides P, Giedzinski E, Limoli CL. Evaluating different routes of extracellular vesicle administration for cranial therapies. *J Cancer Metastasis Treat*. 2020;6(15). doi:10.20517/2394-4722.2020.22

19. Kodali M, Castro OW, Kim DK, et al. Intranasally Administered Human MSC-Derived Extracellular Vesicles Pervasively Incorporate into Neurons and Microglia in both Intact and Status Epilepticus Injured Forebrain. *Int J Mol Sci*. 2019;21(1). doi:10.3390/ijms21010181
20. Dabrowska S, Andrzejewska A, Strzemecki D, Muraca M, Janowski M, Lukomska B. Human bone marrow mesenchymal stem cell-derived extracellular vesicles attenuate neuroinflammation evoked by focal brain injury in rats. *J Neuroinflammation*. 2019;16(1):216. doi:10.1186/s12974-019-1602-5
21. Zhuang X, Xiang X, Grizzle W, et al. Treatment of Brain Inflammatory Diseases by Delivering Exosome Encapsulated Anti-inflammatory Drugs From the Nasal Region to the Brain. *Mol Ther*. 2011;19(10):1769–1779. doi:10.1038/mt.2011.164
22. Monici M. Cell and tissue autofluorescence research and diagnostic applications. *Biotechnol Annu Rev*. 2005;11:227–256. doi:10.1016/S1387-2656(05)11007-2
23. Engel DC, Mies G, Terpolilli NA, et al. Changes of cerebral blood flow during the secondary expansion of a cortical contusion assessed by 14C-iodoantipyrine autoradiography in mice using a non-invasive protocol. *J Neurotrauma*. 2008;25(7):739–753. doi:10.1089/neu.2007.0480
24. Simonsen JB. Pitfalls associated with lipophilic fluorophore staining of extracellular vesicles for uptake studies. *J Extracell Vesicles*. 2019;8(1):1582237. doi:10.1080/20013078.2019.1582237
25. Takov K, Yellon DM, Davidson SM. Confounding factors in vesicle uptake studies using fluorescent lipophilic membrane dyes. *J Extracell Vesicles*. 2017;6(1):1388731. doi:10.1080/20013078.2017.1388731
26. Welsh JA, Goberdhan DCI, O'Driscoll L, et al. Minimal information for studies of extracellular vesicles (MISEV2023): from basic to advanced approaches. *J Extracell Vesicles*. 2024;13(2):e12404. doi:10.1002/jev2.12404